Scattering of surface plasmon polaritons by one-dimensional surface defects

J. Polanco
Computational Science Program, University of Texas, El Paso, Texas 79968, USA

R. M. Fitzgerald
Department of Physics, University of Texas, El Paso, Texas 79968, USA

A. A. Maradudin
Department of Physics and Astronomy and University of California, Irvine, California 92697, USA

(Received 13 December 2012; revised manuscript received 26 February 2013; published 15 April 2013)

The reduced Rayleigh equation for the scattering of a surface plasmon polariton incident normally on a one-dimensional ridge or groove on an otherwise planar metal surface is solved by a purely numerical approach. The solution is used to calculate the reflectivity and transmissivity of the surface plasmon polariton and its conversion into volume electromagnetic waves in the vacuum above the metal surface. The results obtained are compared with those of earlier calculations of these quantities.

DOI: 10.1103/PhysRevB.87.155417 PACS number(s): 71.36.+c

I. INTRODUCTION

There are at least two reasons why the scattering of surface plasmon polaritons by surface defects is of interest in the field of plasmonics.[1] The energy mean free path of a surface plasmon polariton can be decreased by the scattering out of the beam caused by the presence of surface defects, so that it is important for applications of these surface waves to be able to calculate the cross section for such scattering. On the other hand, surface defects of particular forms and sizes can scatter surface plasmon polaritons in desirable ways. For example, they can act as mirrors for surface plasmon polaritons,[2] or as flashlights,[3,4] and can also focus them.[5,6] The ability to control the propagation of surface plasmon polaritons is central to their use in devices. It is therefore important to be able to calculate the scattered field when a surface plasmon polariton is incident on a specified surface defect.

The scattering of surface plasmon polaritons by surface defects of various types has been studied theoretically by several approaches. The scattering from a circularly symmetric protuberance or indentation on an otherwise planar metal surface was investigated by means of a reduced Rayleigh equation.[7] The scattering from a dielectric rectangular parallelepiped on the planar surface of a metal film in the Kretschmann attenuated total reflection geometry[8] was calculated by means of a Green's function method.[9] An effective boundary condition was used in a calculation of the scattering from dielectric defects defined by an anisotropic Gaussian profile and by a hemiellipsoidal profile on a planar metal surface.[10]

The majority of such scattering calculations however, have been devoted to scattering from one-dimensional surface defects, i.e., defects whose profiles are invariant along one of the coordinate axes, such as an isolated groove or ridge. In such studies the scattering of surface plasmon polaritons by defects of various profiles was also investigated by several different approaches. Thus, scattering from an isolated groove or ridge[11–14] or from an array of several parallel grooves or ridges[15] was studied by means of a simple impedance boundary condition.[16] In subsequent studies of scattering from an isolated groove or ridge a more refined impedance boundary condition was employed.[17,18] Two different Green's function methods have also been applied to the solution of the problem, namely a surface integral method[19] and a volume integral method.[20–22] Finally, finite-difference time-domain and boundary-element methods have been used in calculations of the reflection of a surface plasmon polariton from a deep groove.[23]

In this paper we present an approach to the scattering of a surface plasmon polariton incident normally on a one-dimensional nanoscale topographical surface defect on an otherwise planar vacuum-metal defect, that has not been used for this purpose until now, namely the use of the reduced Rayleigh equation.[24] Just as the use of an impedance boundary condition eliminates the electromagnetic field in the metal from consideration, so does the use of the reduced Rayleigh equation. In this method the field in the metal is accounted for through the boundary condition at the interface satisfied by the field in the vacuum. This has the consequence that only a single one-dimensional integral equation has to be solved to obtain the amplitude of the scattered field, in contrast with the pair of coupled one-dimensional integral equations that have to be solved when a Green's function approach is used. The computational problem is simplified thereby. It is a rigorous approach to scattering from defects with surface profile functions for which the Rayleigh hypothesis[25] is valid. This will be discussed later in this paper. In the form used in this paper it is applicable only to lossless metals. This restriction is not a serious one because the surface plasmon polariton energy mean free path is generally longer than the width of a nanoscale surface defect, as will be discussed later in this paper. It is a restriction that can be lifted at the expense of having to solve a more complicated one-dimensional integral equation for the scattering amplitude.

The approach developed in this paper will be applied to the scattering of a surface plasmon polariton from grooves and ridges on an otherwise planar surface defined by Gaussian and triangular surface profile functions. Some of our results will

be compared with those of earlier studies of scattering from such defects.

II. THE SCATTERED FIELD

The system we study consists of vacuum in the region $x_3 > \zeta(x_1)$, and a metal, characterized by an isotropic, frequency-dependent, real dielectric function $\epsilon(\omega)$, in the region $x_3 < \zeta(x_1)$. The surface profile function $\zeta(x_1)$ is assumed to be a single-valued function of x_1 that is differentiable, and is sensibly nonzero over only a finite portion of the x_1 axis about its origin.

A surface plasmon polariton of frequency ω, whose sagittal plane is the x_1x_3 plane, propagates in the $+x_1$ direction along the x_1 axis. The single nonzero component of its magnetic field in the region $x_3 > \zeta(x_1)_{\max}$ is the sum of an incident field and a scattered field:

$$H_2^{>}(x_1,x_3|\omega) = \exp[ik(\omega)x_1 - \beta_0(\omega)x_3] + \int_{-\infty}^{\infty}\frac{dq}{2\pi} \times A(q|k(\omega))\exp[iqx_1 - \beta_0(q,\omega)x_3], \quad (2.1)$$

where

$$k(\omega) = \frac{\omega}{c}\left[\frac{|\epsilon(\omega)|}{|\epsilon(\omega)|-1}\right]^{\frac{1}{2}} \quad (2.2a)$$

$$\beta_0(\omega) = \frac{\omega}{c}\left[\frac{1}{|\epsilon(\omega)|-1}\right]^{\frac{1}{2}} \quad (2.2b)$$

are the wave number of a surface plasmon polariton of frequency ω at a planar vacuum-metal interface and the inverse decay length of its field into the vacuum, respectively. Our notation here indicates that we are working in the frequency range in which $\epsilon(\omega)$ is negative, which is the frequency range in which surface plasmon polaritons exist. The function $\beta_0(q,\omega)$ is defined by

$$\beta_0(q,\omega) = [q^2 - (\omega/c)^2]^{\frac{1}{2}}, \quad \mathrm{Re}\beta_0(q,\omega) > 0, \quad \mathrm{Im}\beta_0(q,\omega) < 0. \quad (2.3)$$

The magnetic field in the region of the metal, $x_3 < \zeta(x_1)_{\min}$, can be written in a similar form:

$$H_2^{<}(x_1,x_3|\omega) = \exp[ik(\omega)x_1 + \beta(\omega)x_3] + \int_{-\infty}^{\infty}\frac{dq}{2\pi} \times B(q|k(\omega))\exp[iqx_1 + \beta(q,\omega)x_3], \quad (2.4)$$

where

$$\beta(\omega) = \frac{\omega}{c}\frac{|\epsilon(\omega)|}{[|\epsilon(\omega)|-1]^{\frac{1}{2}}} \quad (2.5a)$$

$$\beta(q,\omega) = [q^2 - \epsilon(\omega)(\omega/c)^2]^{\frac{1}{2}}, \quad \mathrm{Re}\beta(q,\omega) > 0, \quad \mathrm{Im}\beta(q,\omega) < 0. \quad (2.5b)$$

The boundary conditions satisfied by $H_2^{\gtrless}(x_1,x_3|\omega)$ at the interface $x_3 = \zeta(x_1)$ are the continuity of the tangential components of the magnetic and electric fields across it,

$$H_2^{>}(x_1,x_3|\omega) = H_2^{<}(x_1,x_3|\omega) \quad (2.6a)$$

$$\frac{\partial}{\partial n}H_2^{>}(x_1,x_3|\omega) = \frac{1}{\epsilon(\omega)}\frac{\partial}{\partial n}H_2^{<}(x_1,x_3|\omega), \quad (2.6b)$$

where

$$\frac{\partial}{\partial n} = \frac{1}{[1+(\zeta'(x_1))^2]^{\frac{1}{2}}}\left(-\zeta'(x_1)\frac{\partial}{\partial x_1} + \frac{\partial}{\partial x_3}\right) \quad (2.6c)$$

is the derivative along the normal to the surface at each point of it, directed from the metal toward the vacuum.

When Eqs. (2.1) and (2.4) are substituted into Eqs. (2.6), we obtain a pair of coupled integral equations for the coefficient functions $A(q|k(\omega))$ and $B(q|k(\omega))$:

$$\int_{-\infty}^{\infty}\frac{dq}{2\pi}A(q|k(\omega))\exp[iqx_1 - \beta_0(q,\omega)\zeta(x_1)] - \int_{-\infty}^{\infty}\frac{dq}{2\pi}B(q|k(\omega))\exp[iqx_1 + \beta(q,\omega)\zeta(x_1)] = -\exp[ik(\omega)x_1 - \beta_0(\omega)\zeta(x_1)] + \exp[ik(\omega)x_1 + \beta(\omega)\zeta(x_1)] \quad (2.7a)$$

$$\int_{-\infty}^{\infty}\frac{dq}{2\pi}A(q|k(\omega))[-iq\zeta'(x_1) - \beta_0(q,\omega)]\exp[iqx_1 - \beta_0(q,\omega)\zeta(x_1)] - \frac{1}{\epsilon(\omega)}\int_{-\infty}^{\infty}\frac{dq}{2\pi}B(q|k(\omega))[-iq\zeta'(x_1) + \beta(q,\omega)]\exp[iqx_1 + \beta(q,\omega)\zeta(x_1)] = -[-ik(\omega)\zeta'(x_1) - \beta_0(\omega)]\exp[ik(\omega)x_1 - \beta_0(\omega)\zeta(x_1)] + \frac{1}{\epsilon(\omega)}[-ik(\omega)\zeta'(x_1) + \beta(\omega)]\exp[ik(\omega)x_1 + \beta(\omega)\zeta(x_1)]. \quad (2.7b)$$

However, only the electromagnetic field in the vacuum is experimentally accessible. Therefore we need only the amplitude $A(q|k(\omega))$. A single integral equation for it can be obtained in the following way. We first multiply Eq. (2.7a) by $[ip\zeta'(x_1) + \beta(p,\omega)]\exp[-ipx_1 + \beta(p,\omega)\zeta(x_1)]$ where p is an arbitrary wave number, and then integrate the result with respect to x_1. We then multiply Eq. (2.7b) by $-\epsilon(\omega)\exp[-ipx_1 + \beta(p,\omega)\zeta(x_1)]$ and integrate the result with respect to x_1. We finally add the resulting pair of equations and obtain

$$\int_{-\infty}^{\infty}\frac{dq}{2\pi}\frac{I(\beta(p,\omega)-\beta_0(q,\omega)|p-q)}{\beta(p,\omega)-\beta_0(q,\omega)}[\beta(p,\omega)\beta_0(q,\omega) - pq]A(q|k(\omega)) = -\frac{I(\beta(p,\omega)-\beta_0(\omega)p-k(\omega))}{\beta(p,\omega)-\beta_0(\omega)}[\beta(p,\omega)\beta_0(\omega) - pk(\omega)], \quad (2.8)$$

where we have introduced the function $I(\gamma|Q)$ defined by

$$\exp[\gamma\zeta(x_1)] = \int_{-\infty}^{\infty} \frac{dQ}{2\pi} I(\gamma|Q)\exp(iQx_1). \tag{2.9}$$

It follows from this result that

$$\zeta'(x_1)\exp[\gamma\zeta(x_1)] = \int_{-\infty}^{\infty} \frac{dQ}{2\pi}\frac{iQ}{\gamma} I(\gamma|Q)\exp(iQx_1). \tag{2.10}$$

Both of these relations were used in obtaining Eq. (2.8). For the evaluation of $I(\gamma|Q)$ we need the inverse relation

$$I(\gamma|Q) = \int_{-\infty}^{\infty} dx_1 \exp(-iQx_1)\exp[\gamma\zeta(x_1)]. \tag{2.11}$$

It is convenient to remove a delta function from the function $I(\gamma|Q)$ by rewriting Eq. (2.11) as

$$\begin{aligned} I(\gamma|Q) &= \int_{-\infty}^{\infty} dx_1 \exp(-iQx_1)\{1+\exp[\gamma\zeta(x_1)]-1\} \\ &= 2\pi\delta(Q) + \gamma J(\gamma|Q), \end{aligned} \tag{2.12}$$

where

$$J(\gamma|Q) = \int_{-\infty}^{\infty} dx_1 \exp(-iQx_1)\frac{exp[\gamma\zeta(x_1)]-1}{\gamma}. \tag{2.13}$$

On substituting Eq. (2.12) into Eq. (2.8) we obtain the equation satisfied by $A(q|k(\omega))$ in the form

$$\begin{aligned} &\frac{\epsilon(\omega)\beta_0(p,\omega)+\beta(p,\omega)}{\epsilon(\omega)-1}A(p|k(\omega)) + \int_{-\infty}^{\infty}\frac{dq}{2\pi}J(\beta(p,\omega) \\ &\quad -\beta_0(q,\omega)|p-q)[\beta(p,\omega)\beta_0(q,\omega)-pq]A(q|k(\omega)) \\ &= -J(\beta(p,\omega)-\beta_0(\omega)|p-k(\omega))[\beta(p,\omega)\beta_0(\omega)-pk(\omega)]. \end{aligned} \tag{2.14}$$

The coefficient of $A(p|k(\omega))$ on the left-hand side of this equation vanishes when $p=\pm k(\omega)$, where $k(\omega)$, defined by Eq. (2.2a), is the wave number of the surface plasmon polariton of frequency ω at a planar vacuum-metal interface. This means that $A(p|k(\omega))$ has simple poles at these values of p. In a numerical solution of an integral equation it is preferable for the unknown function being sought to be free from singularities. Consequently, we introduce the function $a(p,\omega)$ by

$$A(p|k(\omega)) = \frac{a(p,\omega)}{\epsilon(\omega)\beta_0(p,\omega)+\beta(p,\omega)}, \tag{2.15}$$

so that $a(p,\omega)$ is free from singularities. The equation satisfied by this function is

$$\begin{aligned} &a(p,\omega) - (\epsilon(\omega)-1)\int_{-\infty}^{\infty}\frac{dq}{2\pi}J(\beta(p,\omega)-\beta_0(q,\omega)|p-q) \\ &\quad\times\frac{pq-\beta(p,\omega)\beta_0(q,\omega)}{\epsilon(\omega)\beta_0(q,\omega)+\beta(q,\omega)}a(q,\omega) \\ &= (\epsilon(\omega)-1)J(\beta(p,\omega)-\beta_0(\omega)|p-k(\omega)) \\ &\quad\times[pk(\omega)-\beta(p,\omega)\beta_0(\omega)]. \end{aligned} \tag{2.16}$$

This is the equation that will be solved numerically.

The magnetic field in the vacuum region scattered by the surface defect is given by the second term on the right-hand side of Eq. (2.1). When the expression for $A(q|k(\omega))$ obtained from Eq. (2.15) is substituted into Eq. (2.1), the scattered field becomes

$$H_2^>(x_1,x_3|\omega)_{\rm sc} = \int_{-\infty}^{\infty}\frac{dq}{2\pi}\frac{e^{iqx_1-\beta_0(q,\omega)x_3}}{\epsilon(\omega)\beta_0(q,\omega)+\beta(q,\omega)}a(q,\omega). \tag{2.17}$$

The surface plasmon polariton contribution to this field is given by the residues at the poles of the integrand at $q=\pm k(\omega)$. In the vicinity of these poles we find that

$$\begin{aligned} &\frac{1}{\epsilon(\omega)\beta_0(q,\omega)+\beta(q,\omega)} \\ &\quad= \frac{\epsilon(\omega)\beta_0(\omega)}{[\epsilon^2(\omega)-1]k(\omega)}\frac{1}{q-k(\omega)} \qquad q\approx k(\omega) \qquad (2.18a) \\ &\quad= -\frac{\epsilon(\omega)\beta_0(\omega)}{[\epsilon^2(\omega)-1]k(\omega)}\frac{1}{q+k(\omega)} \qquad q\approx -k(\omega). \qquad (2.18b) \end{aligned}$$

We now give $\epsilon(\omega)$ an infinitesimal positive imaginary part to define how the poles at $q=\pm k(\omega)$ are to be dealt with. This results in $k(\omega)$ acquiring an infinitesimal positive imaginary part. The integral over q in Eq. (2.17) is then evaluated by going into the complex q plane in the manner this was done in Ref. 19, and employing the residue theorem. The result is

$$\begin{aligned} &H_2^>(x_1,x_3|\omega)_{\rm sc,spp} \\ &= i\frac{\epsilon(\omega)\beta_0(\omega)}{[\epsilon^2(\omega)-1]k(\omega)}\exp[ik(\omega)x_1-\beta_0(\omega)x_3]a(k(\omega),\omega) \\ &\qquad x_1>0 \qquad (2.19a) \\ &= i\frac{\epsilon(\omega)\beta_0(\omega)}{[\epsilon^2(\omega)-1]k(\omega)}\exp[-ik(\omega)x_1-\beta_0(\omega)x_3]a(-k(\omega),\omega) \\ &\qquad x_1<0. \qquad (2.19b) \end{aligned}$$

Consequently, the transmitted surface plasmon polariton field is

$$\begin{aligned} H_2^>(x_1,x_3|\omega)_{\rm tr,spp} &= \left[1+i\frac{\epsilon(\omega)}{\epsilon^2(\omega)-1}\frac{\beta_0(\omega)}{k(\omega)}a(k(\omega),\omega)\right] \\ &\quad\times\exp[ik(\omega)x_1-\beta_0(\omega)x_3] \quad x_1>0. \end{aligned} \tag{2.20}$$

The first term on the right-hand side of this equation is the contribution from the incident field, which is present even in the absence of the surface defect. The reflected surface plasmon polariton field is

$$\begin{aligned} H_2^>(x_1,x_3|\omega)_{\rm ref,spp} &= i\frac{\epsilon(\omega)}{\epsilon^2(\omega)-1}\frac{\beta_0(\omega)}{k(\omega)}a(-k(\omega),\omega) \\ &\quad\times\exp[-ik(\omega)x_1-\beta_0(\omega)x_3] \quad x_1<0. \end{aligned} \tag{2.21}$$

The factor $\epsilon(\omega)\beta_0(\omega)/\{[\epsilon^2(\omega)-1]k(\omega)\}$ can be simplified to

$$\frac{\epsilon(\omega)}{\epsilon^2(\omega)-1}\frac{\beta_0(\omega)}{k(\omega)} = -\frac{|\epsilon(\omega)|^{\frac{1}{2}}}{\epsilon^2(\omega)-1}. \tag{2.22}$$

III. THE REFLECTION, TRANSMISSION, AND RADIATION COEFFICIENTS

To calculate the reflection, transmission, and radiation coefficients we need first of all the total time-averaged incident

flux crossing the plane $x_1 = -c$ to the left of the surface defect, where the vacuum-dielectric interface is planar. It is given by

$$\langle S_1\rangle = -\frac{c}{8\pi}\mathrm{Re}\int_{-\infty}^{\infty} dx_3 E_3(-c,x_3|\omega)H_2^*(-c,x_3|\omega), \tag{3.1}$$

where S_1 is the 1-Cartesian component of the Poynting vector, and the angle brackets denote a time average. In p polarization we have

$$E_3(x_1,x_3|\omega) = i\frac{c}{\omega\epsilon}\frac{\partial}{\partial x_1}H_2(x_1,x_3|\omega), \tag{3.2}$$

where ϵ is the dielectric constant of the medium in which the field is being calculated. Thus, we have

$$\langle S_1\rangle = \frac{c^2}{8\pi\omega}\mathrm{Im}\int_{-\infty}^{\infty} dx_3 \frac{1}{\epsilon}\frac{\partial}{\partial x_1}H_2(-c,x_3|\omega)H_2^*(-c,x_3|\omega). \tag{3.3}$$

The incident magnetic field can be written as

$$H_2^{>}(-c,x_3|\omega)_{\mathrm{inc}} = \exp[-ik(\omega)c - \beta_0(\omega)x_3] \quad x_3 > 0 \tag{3.4a}$$

$$H_2^{<}(-c,x_3|\omega)_{\mathrm{inc}} = \exp[-ik(\omega)c + \beta(\omega)x_3] \quad x_3 < 0. \tag{3.4b}$$

Consequently, we have

$$\begin{aligned}\langle S_1\rangle_{\mathrm{inc}} &= \frac{c^2}{8\pi\omega}\mathrm{Im}\int_0^{\infty} dx_3 ik(\omega)\exp[-2\beta_0(\omega)x_3] \\ &\quad + \frac{c^2}{8\pi\omega\epsilon(\omega)}\mathrm{Im}\int_{-\infty}^{0} dx_3 ik(\omega)\exp[2\beta(\omega)x_3] \\ &= \frac{c^2}{16\pi\omega}\frac{k(\omega)}{\beta_0(\omega)}\left(1-\frac{1}{\epsilon^2(\omega)}\right).\end{aligned} \tag{3.5}$$

The reflected surface plasmon polariton field at $x_3 = -c$ can be written as

$$H_2^{>}(-c,x_3|\omega)_{\mathrm{ref}} = r(\omega)\exp[ik(\omega)c - \beta_0(\omega)x_3] \quad x_3 > 0 \tag{3.6a}$$

$$H_2^{<}(-c,x_3|\omega)_{\mathrm{ref}} = r(\omega)\exp[ik(\omega)c + \beta(\omega)x_3] \quad x_3 < 0, \tag{3.6b}$$

where

$$r(\omega) = -i\frac{|\epsilon(\omega)|^{\frac{1}{2}}}{\epsilon^2(\omega)-1}a(-k(\omega),\omega). \tag{3.7}$$

The total time-averaged flux of the reflected field is obtained from Eq. (3.3) in the form

$$\begin{aligned}\langle S_1\rangle_{\mathrm{ref}} &= \frac{c^2}{8\pi\omega}\mathrm{Im}\int_0^{\infty} dx_3(-i)k(\omega)|r(\omega)|^2\exp[-2\beta_0(\omega)x_3] \\ &\quad + \frac{c^2}{8\pi\omega\epsilon(\omega)}\mathrm{Im}\int_{-\infty}^{0} dx_3(-i)k(\omega)|r(\omega)|^2 \\ &\quad \times\exp[2\beta(\omega)x_3] \\ &= -\frac{c^2}{16\pi\omega}\frac{k(\omega)}{\beta_0(\omega)}|r(\omega)|^2\left(1-\frac{1}{\epsilon^2(\omega)}\right).\end{aligned} \tag{3.8}$$

The reflectivity of the surface plasmon polariton is therefore

$$\begin{aligned}R(\omega) &= \frac{|\langle S_1\rangle_{\mathrm{ref}}|}{\langle S_1\rangle_{\mathrm{inc}}} = |r(\omega)|^2 \\ &= \frac{|\epsilon(\omega)|}{[\epsilon^2(\omega)-1]^2}|a(-k(\omega),\omega)|^2.\end{aligned} \tag{3.9}$$

To obtain the transmissivity of the surface plasmon polariton, we need the total time-averaged flux crossing the plane $x_1 = c$ to the right of the surface defect, where the vacuum-metal interface is planar. The transmitted magnetic field can be written as

$$H_2^{>}(c,x_3|\omega)_{\mathrm{tr,spp}} = [1+t(\omega)]\exp[ik(\omega)c - \beta_0(\omega)x_3] \quad x_3 > 0 \tag{3.10a}$$

$$H_2^{<}(c,x_3|\omega)_{\mathrm{tr,spp}} = [1+t(\omega)]\exp[ik(\omega)c + \beta(\omega)x_3] \quad x_3 < 0, \tag{3.10b}$$

where

$$t(\omega) = -i\frac{|\epsilon(\omega)|^{\frac{1}{2}}}{\epsilon^2(\omega)-1}a(k(\omega),\omega). \tag{3.11}$$

Thus, the total time-averaged flux of the transmitted field is obtained from Eq. (3.3) as

$$\begin{aligned}\langle S_1\rangle_{\mathrm{tr}} &= \frac{c^2}{8\pi\omega}|[1+t(\omega)]|^2\mathrm{Im}\int_0^{\infty} dx_3 ik(\omega)\exp[-2\beta_0(\omega)x_3] \\ &\quad + \frac{c^2}{8\pi\omega\epsilon(\omega)}|[1+t(\omega)]|^2 \\ &\quad \times\mathrm{Im}\int_{-\infty}^{0} dx_3 ik(\omega)\exp[2\beta(\omega)x_3] \\ &= \frac{c^2}{16\pi\omega}|[1+t(\omega)]|^2\frac{k(\omega)}{\beta_0(\omega)}\left(1-\frac{1}{\epsilon^2(\omega)}\right).\end{aligned} \tag{3.12}$$

The transmissivity of the surface plasmon polaritons is therefore

$$T(\omega) = \frac{\langle S_1\rangle_{\mathrm{tr}}}{\langle S_1\rangle_{\mathrm{inc}}} = |[1+t(\omega)]|^2. \tag{3.13}$$

To calculate the fraction of the total time-averaged incident flux that is converted into volume electromagnetic waves in the vacuum propagating away from the metal surface, we begin by rewriting the scattered field, Eq. (2.17), in the form

$$H_2^{>}(x_1,x_3|\omega)_{\mathrm{sc}} = i\int_{-\infty}^{\infty}\frac{dq}{2\pi}\frac{\exp[iqx_1 + i\alpha_0(q,\omega)x_3]}{\epsilon(\omega)\alpha_0(q,\omega)+\alpha(q,\omega)}a(q,\omega), \tag{3.14}$$

where

$$\begin{aligned}&\alpha_0(q,\omega) = i\beta_0(q,\omega) = [(\omega/c)^2 - q^2]^{\frac{1}{2}} \\ &\mathrm{Re}\alpha_0(q,\omega) > 0, \quad \mathrm{Im}\alpha_0(q,\omega) > 0\end{aligned} \tag{3.15}$$

and

$$\begin{aligned}&\alpha(q,\omega) = i\beta(q,\omega) = [\epsilon(\omega)(\omega/c)^2 - q^2]^{\frac{1}{2}} \\ &\mathrm{Re}\alpha(q,\omega) > 0, \quad \mathrm{Im}\alpha(q,\omega) > 0.\end{aligned} \tag{3.16}$$

We now need the total time-averaged scattered flux crossing the plane $x_3 = c$ above the metal. It is obtained from the 3-Cartesian component of the Poynting vector of the scattered

field,

$$\langle S_3\rangle = \frac{c}{8\pi}\mathrm{Re}\int_{-\infty}^{\infty} dx_1 E_1(x_1,c|\omega)H_2^*(x_1,c|\omega). \quad (3.17)$$

In p polarization we have

$$E_1(x_1,x_3|\omega) = -i\frac{c}{\omega\epsilon}\frac{\partial}{\partial x_3}H_2(x_1,x_3|\omega), \quad (3.18)$$

where ϵ is the dielectric constant of the medium in which the field is being calculated. Thus, we have

$$\langle S_3\rangle = \frac{c^2}{8\pi\omega}\mathrm{Im}\int_{-\infty}^{\infty} dx_1 \frac{1}{\epsilon}\frac{\partial}{\partial x_3}H_2(x_1,c|\omega)H_2^*(x_1,c|\omega). \quad (3.19)$$

Upon substituting Eq. (3.14) into Eq. (3.19) we obtain

$$\begin{aligned}\langle S_3\rangle_{\mathrm{rad}} &= \frac{c^2}{8\pi\omega}\mathrm{Im}\int_{-\infty}^{\infty} dx_1 \int_{-\infty}^{\infty}\frac{dq}{2\pi}\frac{i\alpha_0(q,\omega)a(q,\omega)}{\epsilon(\omega)\alpha_0(q,\omega)+\alpha(q,\omega)} \\ &\quad\times\int_{-\infty}^{\infty}\frac{dq'}{2\pi}\frac{a^*(q',\omega)}{\epsilon(\omega)\alpha_0^*(q',\omega)+\alpha^*(q',\omega)} \\ &\quad\times e^{i(q-q')x_1+i[\alpha_0(q,\omega)-\alpha_0^*(q',\omega)]x_3} \\ &= \frac{c^2}{8\pi\omega}\mathrm{Im}\int_{-\infty}^{\infty}\frac{dq}{2\pi}i\alpha_0(q,\omega)\left|\frac{a(q,\omega)}{\epsilon(\omega)\alpha_0(q,\omega)+\alpha(q,\omega)}\right|^2 \\ &\quad\times\exp[-2\mathrm{Im}\alpha_0(k,\omega)x_3] \\ &= \frac{c^2}{8\pi\omega}\int_{-\frac{\omega}{c}}^{\frac{\omega}{c}}\frac{dq}{2\pi}\alpha_0(q,\omega)\left|\frac{a(q,\omega)}{\epsilon(\omega)\alpha_0(q,\omega)+\alpha(q,\omega)}\right|^2. \end{aligned} \quad (3.20)$$

It is convenient now to make the change of variable $q = (\omega/c)\sin\theta_s$, which yields

$$\langle S_3\rangle_{\mathrm{rad}} = \int_{-\frac{\pi}{2}}^{\frac{\pi}{2}} d\theta_s P_{\mathrm{rad}}(\theta_s), \quad (3.21)$$

where

$$\begin{aligned}P_{\mathrm{rad}}(\theta_s) &= \frac{\omega}{16\pi^2}\cos^2\theta_s\left|\left[\frac{a(q,\omega)}{\epsilon(\omega)\alpha_0(q,\omega)+\alpha(q,\omega)}\right]_{q=\frac{\omega}{c}\sin\theta_s}\right|^2 \\ &= \frac{c^2}{16\pi^2\omega}\cos^2\theta_s\frac{|a((\omega/c)\sin\theta_s,\omega)|^2}{[\epsilon(\omega)\cos\theta+(\epsilon(\omega)-\sin^2\theta_s)^{\frac{1}{2}}]^2}. \end{aligned} \quad (3.22)$$

The fraction of the incident flux that is radiated into the angular interval $(\theta_s,\theta_s+d\theta_s)$ is then given by

$$\begin{aligned}\langle S(\theta_s)\rangle &= \frac{P_{\mathrm{rad}}(\theta_s)}{\langle S_1\rangle_{\mathrm{inc}}} = \frac{1}{\pi}\frac{|\epsilon(\omega)|}{\epsilon^2(\omega)-1} \\ &\quad\times\cos^2\theta_s\frac{|a((\omega/c)\sin\theta_s,\omega)|^2}{[\epsilon(\omega)\cos\theta_s+(\epsilon(\omega)-\sin^2\theta_s)^{\frac{1}{2}}]^2}. \end{aligned} \quad (3.23)$$

IV. THE NUMERICAL SOLUTION OF EQUATION (2.16)

In solving Eq. (2.16) numerically we begin by noting that $\beta_0(q,\omega)$ is purely imaginary for $|q| < (\omega/c)$ and is purely real for $|q| > (\omega/c)$. Because we work in the frequency range in which $\epsilon(\omega)$ is negative, and because we have assumed that it is real, $\beta(q,\omega)$ is real for all values of q. The infinite region of integration is then truncated to the finite region $(-Q,Q)$, where Q is typically in the range $6(\omega/c)-7(\omega/c)$. We consider the integration of a function $f(p|q)a(q)$ with respect to q over this region.

The interval $[-(\omega/c),(\omega/c)]$ is divided into $2N+1$ subintervals, each of width $\Delta q_1 = 2(\omega/c)/(2N+1)$, so that

$$\int_{-\frac{\omega}{c}}^{\frac{\omega}{c}} dq f(p|q)a(q) = \sum_{n=-N}^{N}\int_{(n-\frac{1}{2})\Delta q_1}^{(n+\frac{1}{2})\Delta q_1} dq f(p|q)a(q), \quad (4.1)$$

where

$$\begin{aligned}f(p|q) &= \frac{\epsilon(\omega)-1}{2\pi}J(\beta(p,\omega)-\beta_0(q,\omega)|p-q) \\ &\quad\times\frac{pq-\beta(p,\omega)\beta_0(q,\omega)}{\epsilon(\omega)\beta_0(q,\omega)+\beta(q,\omega)}. \end{aligned} \quad (4.2)$$

We assume that $a(q,\omega)$ is a slowly varying function of q within each subinterval. We therefore evaluate it at the midpoint of each subinterval and remove it from the integral. In this way we obtain

$$\begin{aligned}\int_{-\frac{\omega}{c}}^{\frac{\omega}{c}} dq f(p|q)a(q) &\cong \sum_{n=-N}^{N} a(n\Delta q_1)\int_{(n-\frac{1}{2})\Delta q_1}^{(n+\frac{1}{2})\Delta q_1} dq f(p|q) \\ &\cong \Delta q_1\sum_{n=-N}^{N} f(p|n\Delta q_1)a(n\Delta q_1). \end{aligned} \quad (4.3)$$

This is essentially the extended midpoint rule. It should be noted that as the frequency ω is changed,so is the integration grid,i.e.,so is Δq_1.

In the interval $(\omega/c) < q < Q$ we have to proceed more carefully,because $f(p|q)$ has a simple pole at $q = k(\omega) > (\omega/c)$. We define a new integration mesh Δq_2 in this interval by $k(\omega)-(\omega/c) = (m^*+\frac{1}{2})\Delta q_2$, where m^* is an integer. The choice $m^* = 1$ is a reasonable one, since $k(\omega)-(\omega/c)$ is typically of the order of $0.05(\omega/c)-0.06(\omega/c)$. If we then assume that the difference $Q-(\omega/c) \approx 5(\omega/c)$ can be written as $Q-(\omega/c) = (M+1)\Delta q_2$, this fixes the value of M at approximately 125.

The integral we have to evaluate now becomes

$$\begin{aligned}\int_{\frac{\omega}{c}}^{Q} dq f(p|q)a(q) &= \sum_{\substack{m=0\\ m\neq m^*}}^{M}\int_{\frac{\omega}{c}+m\Delta q_2}^{\frac{\omega}{c}+(m+1)\Delta q_2} dq f(p|q)a(q) \\ &\quad+\int_{\frac{\omega}{c}+m^*\Delta q_2}^{\frac{\omega}{c}+(m^*+1)\Delta q_2} f(p|q)a(q). \end{aligned} \quad (4.4)$$

We have separated the contribution from the interval $(\omega/c+m^*\Delta q_2, \omega/c+(m^*+1)\Delta q_2)$ because it is in this interval that $f(p|q)$ has a simple pole and can be written as

$$f(p|q) = \frac{g^{(+)}(p|q)}{q-k(\omega)}, \quad (4.5)$$

where

$$g^{(+)}(p|q) = \frac{1}{2\pi} J(\beta(p,\omega) - \beta_0(q,\omega)|p-q) \times \frac{[pq - \beta(p,\omega)\beta_0(q,\omega)][\epsilon(\omega)\beta_0(q,\omega) - \beta(q,\omega)]}{[\epsilon(\omega)+1][q+k(\omega)]}. \tag{4.6}$$

If we give $\epsilon(\omega)$ an infinitesimal positive imaginary part only in the denominator of Eq. (4.5), so that $k(\omega)$ acquires an infinitesimal positive imaginary part, Eq. (4.4) becomes

$$\begin{aligned}\int_{\frac{\omega}{c}}^{Q} dq f(p|q)a(q) \cong & \sum_{\substack{m=0\\ m\neq m^*}}^{M} a\left((\omega/c)+\left(m+\frac{1}{2}\right)\Delta q_2\right) \\ & \times \int_{\frac{\omega}{c}+m\Delta q_2}^{\frac{\omega}{c}+(m+1)\Delta q_2} dq f(p|q) \\ & + a\left((\omega/c)+\left(m^*+\frac{1}{2}\right)\Delta q_2\right) \\ & \times \int_{\frac{\omega}{c}+m^*\Delta q_2}^{\frac{\omega}{c}+(m^*+1)\Delta q_2} dq g^{(+)}(p|q) \\ & \times \left[\frac{1}{(q-k(\omega))_P} + i\pi\delta(q-k(\omega))\right].\end{aligned} \tag{4.7}$$

The notation $(1/x)_P$ denotes the principal part of $(1/x)$, namely $(1/x)_P = \lim_{\eta\to 0+}(x/(x^2+\eta^2))$. If we recall that $(\omega/c)+(m^*+\frac{1}{2})\Delta q_2 = k(\omega)$, this result can be rewritten as

$$\begin{aligned}\int_{\frac{\omega}{c}}^{Q} dq f(p|q)a(q) = & \Delta q_2 \sum_{\substack{m=0\\ m\neq m^*}}^{M} f\left(p|(\omega/c)+\left(m+\frac{1}{2}\right)\Delta q_2\right) \\ & \times a\left((\omega/c)+\left(m+\frac{1}{2}\right)\Delta q_2\right) \\ & + a(k(\omega)) \int_{k(\omega)-\frac{1}{2}\Delta q_2}^{k(\omega)+\frac{1}{2}\Delta q_2} \frac{g^{(+)}(p|q) - g^{(+)}(p|k(\omega))}{q-k(\omega)} \\ & + i\pi g^{(+)}(p|k(\omega))a(k(\omega)).\end{aligned} \tag{4.8}$$

The integral in this expression has no singularity and is evaluated using a fine mesh.

The integral over the interval $-Q < q < -(\omega/c)$ is treated in the same way, with the result

$$\begin{aligned}\int_{-Q}^{-\frac{\omega}{c}} dq f(p|q)a(q) \cong & \Delta q_2 \sum_{\substack{m=0\\ m\neq m^*}}^{M} f\left(p|-(\omega/c)-\left(m+\frac{1}{2}\right)\Delta q_2\right) \\ & \times a\left(-(\omega/c)-\left(m+\frac{1}{2}\right)\Delta q_2\right) - a(-k(\omega)) \\ & \times \int_{k(\omega)-\frac{1}{2}\Delta q_2}^{k(\omega)+\frac{1}{2}\Delta q_2} dq \frac{g^{(-)}(p|-q) - g^{(-)}(p|-k(\omega))}{q-k(\omega)} \\ & - i\pi g^{(-)}(p|-k(\omega))a(-k(\omega)),\end{aligned} \tag{4.9}$$

where

$$g^{(-)}(p|q) = \frac{1}{2\pi} J(\beta(p,\omega) - \beta_0(q,\omega)|p-q) \times \frac{[pq - \beta(p,\omega)\beta_0(q,\omega)][\epsilon(\omega)\beta_0(q,\omega) - \beta(q,\omega)]}{[\epsilon(\omega)+1][q-k(\omega)]}. \tag{4.10}$$

When the wave number p is given the discrete values that q takes in the three integration domains, a $[2(N+M)+3] \times [2(N+M)+3]$ matrix equation is obtained for the values of the function $a(q,\omega)$ at these values of q. From this equation the functions $a(\pm k(\omega))$ are obtained because $\pm k(\omega)$ are among the $2(N+M)+3$ values q takes in evaluating the integral in Eq. (2.16).

V. RESULTS

To illustrate the preceding results we have calculated the reflection and transmission of a surface plasmon polariton incident normally on a ridge or groove on an otherwise planar silver surface, and its conversion into volume electromagnetic waves in the vacuum. The dielectric function for silver was assumed to have the free electron form

$$\epsilon(\omega) = 1 - \frac{\omega_p^2}{\omega^2}, \tag{5.1}$$

with a value of the plasma frequency given by $\omega_p = 11.76 \times 10^{15}\ \mathrm{s}^{-1}$. This value was obtained from the value of the surface impedance $\xi = [\epsilon(\omega)]^{-\frac{1}{2}} = -0.227i$ at a wavelength $\lambda = 600$ nm used by Nikitin, López-Tejeira, and Martín-Moreno[17] in their study of the scattering of a surface plasmon polariton by a one-dimensional defect on a silver surface. Our choice of this value makes possible a comparison of some of our results with some of theirs.

In our first illustrative example the surface profile function $\zeta(x_1)$ is assumed to have the Gaussian form

$$\zeta(x_1) = A\exp\left(-x_1^2/R^2\right). \tag{5.2}$$

It describes a ridge when A is positive, and a groove when A is negative. The function $J(\gamma|Q)$ corresponding to this profile function is

$$J(\gamma|Q) = \frac{\sqrt{\pi}R}{\gamma} \sum_{n=1}^{\infty} \frac{(\gamma A)^n}{\sqrt{n}n!} \exp\left(-\frac{R^2Q^2}{4n}\right). \tag{5.3}$$

For the values of A and R used in the present calculations, no more than the first 20 terms in this expansion were needed to obtain converged results.

We consider first the frequency dependence of the transmittance $T(\omega)$, the reflectance $R(\omega)$, and the emittance $S(\omega)$, when a surface plasmon polariton is incident on the groove or ridge defined by Eq. (5.2) whose $1/e$ half width R is fixed at $R = 250$ nm, while its amplitude A is given the values $A = \pm 40$ nm, ± 60 nm, and ± 80 nm. The spectral range within which these

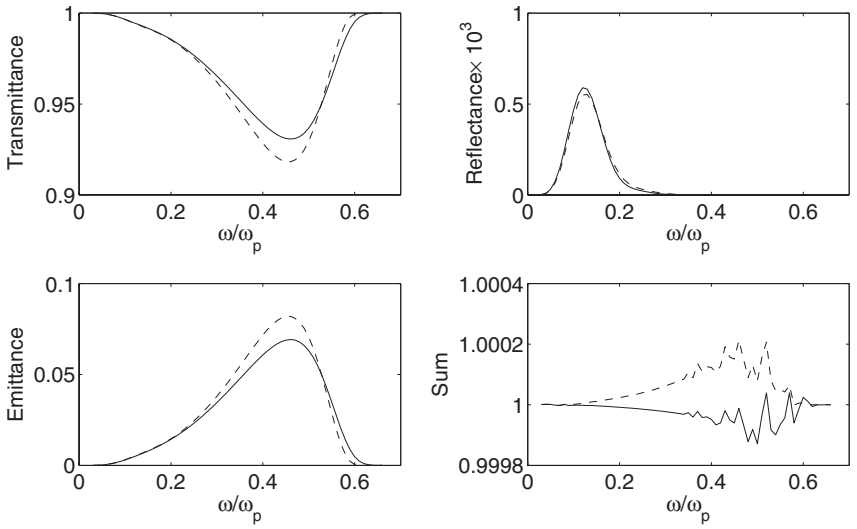

FIG. 1. The frequency dependence of the transmittance, reflectance, emittance, and their sum, when a surface plasmon polariton is incident normally on a Gaussian surface defect, defined by Eq. (5.2), on an otherwise planar silver surface. The values of the parameters assumed in obtaining these results are $\omega_p = 11.76 \times 10^{15}\ \mathrm{s}^{-1}$, $R = 250$ nm, and $A = 40$ nm (——) and $A = -40$ nm(- - - -).

functions are calculated is $0 < \omega < \omega_p/\sqrt{2}$, i.e., the range within which a surface plasmon polariton at a vacuum-free electron metal interface exists.

In Fig. 1 we present plots of $T(\omega), R(\omega), S(\omega)$, and the sum $R(\omega) + S(\omega) + T(\omega)$ as functions of frequency for a defect defined by $A = \pm 40$ nm. The transmittance $T(\omega)$ has a single minimum for both a ridge and a groove, and the emittance $S(\omega)$ has a single maximum for both surface profiles, as does the reflectance $R(\omega)$. We see from these results that the reflectance is smaller than the transmittance and emittance by a factor of about one thousand. The differences between the values of $T(\omega), R(\omega)$, and $S(\omega)$ for a ridge and a groove are not large. The minimum value of the transmittance is larger for a ridge than for a groove, the maximum value of the emittance is smaller for a ridge than for a groove, and the maximum value of the reflectance is larger for the ridge than for the groove. Finally, unitarity (energy conservation) is satisfied with an error smaller than approximately 0.02%. Although this is a necessary condition for the correctness of our results, its satisfaction does not guarantee their correctness.

When the amplitude of the surface defect is increased to $|A| = 60$ nm (Fig. 2), the results for $T(\omega), R(\omega), S(\omega)$, and their sum are qualitatively similar to those presented in Fig. 1. However, there are some quantitative differences. The minima in the transmittance of both a ridge and a groove occur at smaller values of this function, but the minimum value of the transmittance is again larger for a ridge than for a groove. The maxima in the emittance and reflectance of both a ridge and a groove occur at larger values of these functions. However, the maximum value of the emittance is larger for a groove than for a ridge, while the maximum value of the reflectance is larger for the ridge than for the groove. These characteristics of the frequency dependencies of the transmittance, emittance, and reflectance are maintained when the amplitude of the surface defect is increased to $|A| = 80$ nm (Fig. 3).

It should be noted that unitarity is satisfied with an error smaller than about 0.025–0.5%. in all of the cases considered. Moreover, the frequency at which the maxima and minima of the transmittance, emittance, and reflectance occur is almost unaffected by changes in $|A|$ as R remains fixed, and has the value $\omega/\omega_p \cong 0.45$ in all of the cases considered.

We now turn to the angular distribution of the emittance, $S(\theta_s)$. We assume that the frequency of the incident surface plasmon polariton is $\omega/\omega_p = 0.267$, which corresponds to a wavelength $\lambda = 600$ nm. The $1/e$ half width of the surface defect is fixed at a value $R = 250$ nm, while the amplitude A

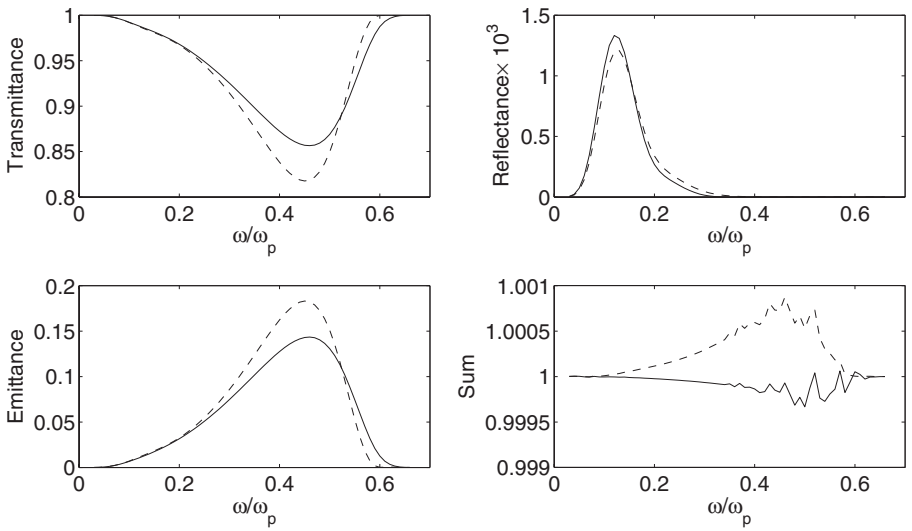

FIG. 2. The same as Fig. 1, but for $|A| = 60$ nm.

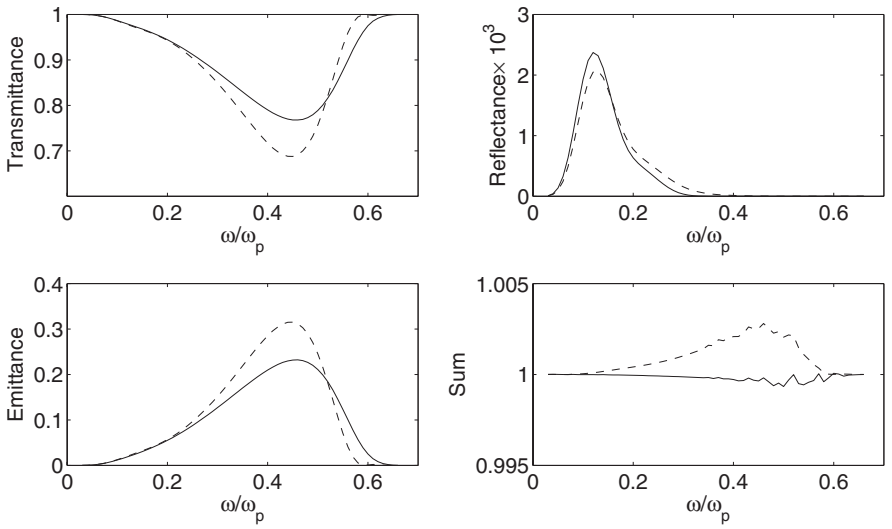

FIG. 3. The same as Fig. 1, but for $|A| = 80$ nm.

of the defect takes the values $A = 12$, 40, 60, and 80 nm for the case of a ridge, and the values $A = -12, -40, -60$, and -80 nm for the case of a groove. The results are presented in Fig. 4.

Two principal results can be obtained from the figure. The first is that a groove converts more of the energy in the incident surface plasmon polariton into volume electromagnetic waves in the vacuum than does a ridge, for each value of $|A|$. The second is that for all the values of $|A|$ for which Fig. 4 was calculated, the radiation pattern has a maximum at a scattering angle $\theta_s = 30^\circ$. We will return to this result later in this section.

Until now we have considered spectral dependencies of the transmittance, emittance, and reflectance when the width of the surface defect is fixed and its amplitude is varied. We now consider the transmittance, emittance, and reflectance of the surface defect as functions of its width when its amplitude

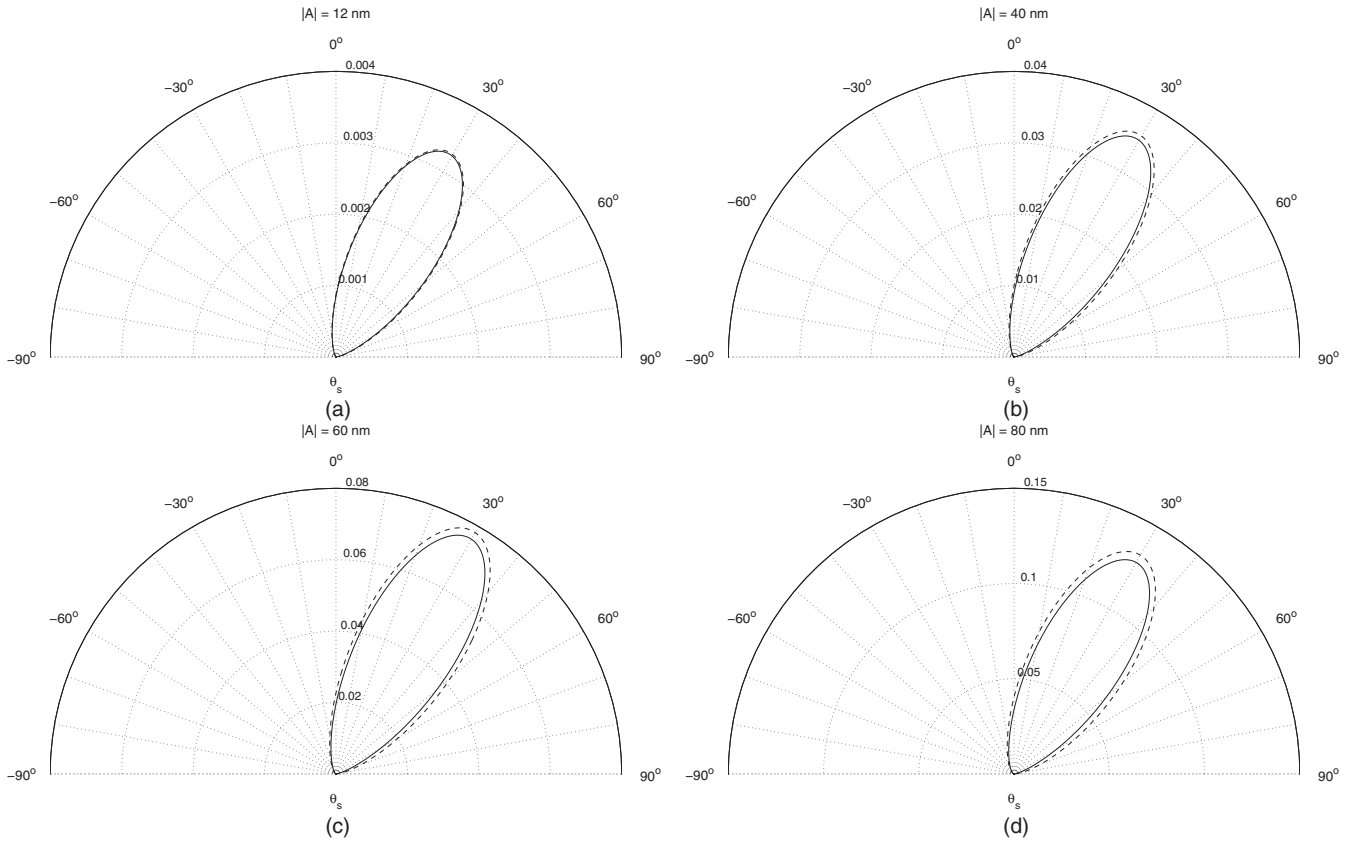

FIG. 4. The angular dependence of the emittance when a surface plasmon polariton whose wavelength is $\lambda = 600$ nm is incident normally on a Gaussian surface defect, defined by Eq. (5.2), on an otherwise planar silver surface. The values of the parameters assumed in obtaining these results are $\omega_p = 11.76 \times 10^{15}$ s^{-1}, $R = 250$ nm, and $|A| = \pm 12$ nm (a), ± 40 nm (b), ± 60 nm (c), and ± 80 nm (d). In each case the solid curve depicts the result for a ridge, while the dashed curve depicts the result for a groove.

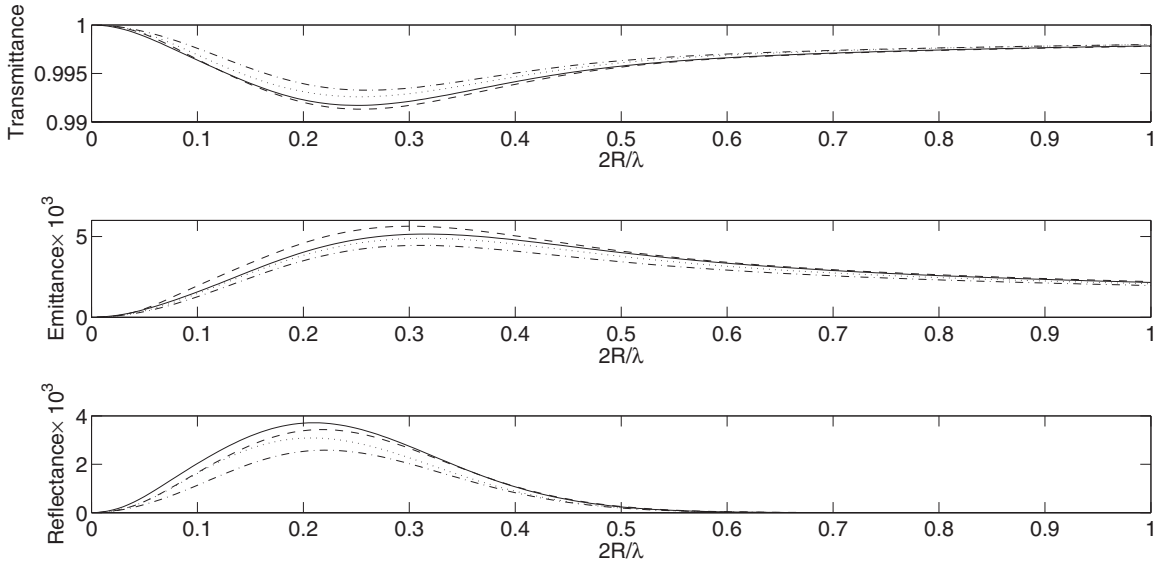

FIG. 5. The dependence of the transmittance, reflectance, and emittance of a Gaussian ridge or groove on an otherwise planar silver surface on $2R/\lambda$, when a surface plasmon polariton whose wavelength is $\lambda = 600$ nm is incident normally on it. The amplitude of the defect is $|A| = 12$ nm. The solid (——) and dashed (- - - -) curves in each case depict the results for a ridge and a groove, respectively, obtained by the approach of this paper. The dotted ($\cdot\ \cdot\ \cdot$) and the dash-dotted ($-\ \cdot\ -\ \cdot$) curves in each case depict the results for a ridge and a groove, respectively, obtained in Ref. 17.

is fixed, as is the wavelength of the incident surface plasmon polariton. In Fig. 5 we present plots of these functions versus $2R/\lambda$, in the interval $0 \leqslant 2R/\lambda \leqslant 1$, when the frequency of the surface plasmon polariton is $\omega/\omega_p = 0.267$ ($\lambda = 600$ nm), while the amplitude of the surface defect is $|A| = 12$ nm. Four curves are presented for each function. The solid curve (——) and the dashed curve (- - - - -) in each case depict the results obtained for a ridge and a groove, respectively, by the approach of this paper. The dotted curve ($\cdot\ \cdot\ \cdot\ \cdot\ \cdot$) and the dashed-dotted curve ($-\ \cdot\ -\ \cdot\ -\ \cdot$) in each case depict the results for a ridge and a groove, respectively, calculated by Nikitin, López-Tejeira, and Martín-Moreno. It should be noted that the width a of the Gaussian defect in Ref. 17 is $2R$ in our notation. While the results for the ridge obtained by the two approaches are in quite good agreement, the results for a groove agree less well.

Finally, in Fig. 6 we consider the angular dependence of the emittance, $S(\theta_s)$, when a surface plasmon polariton whose wavelength is $\lambda = 600$ nm is incident normally on a Gaussian groove defined by Eq. (5.2). The value of the parameter A assumed in obtaining the results presented in this figure is $A = -12$ nm, while $2R/\lambda$ takes the values (a) 0.1, (b) 0.25, (c) 0.5, (d) 0.6, and (e) 0.8. In each case the solid curve depicts the result obtained by the approach of this paper, while the dashed curve depicts the result obtained in Ref. 17. Both sets of results show that for small values of $2R/\lambda$ the radiation is predominantly in the backward direction. However, for values of $2R/\lambda$ larger than approximately 0.5 the radiation is predominantly in the forward direction. Thus, one can modify the radiation pattern in useful ways by increasing R for a fixed value of $-A$.

When we compare the results presented in Figs. 4 and 6 we see that it is varying the width of the groove while keeping its depth fixed that controls the scattering angle at which the maximum scattered intensity occurs. Keeping the width of the groove fixed while increasing its depth does not change the scattering angle at which the maximum scattered intensity occurs.

The results obtained by both approaches are qualitatively similar. However, the results obtained by the use of an impedance boundary condition[17] are systematically smaller than those obtained by the approach presented in this paper. This is also reflected in the results for the emittance in the scattering from a groove presented in Fig. 5. The results shown in Figs. 5 and 6 give an indication of the accuracy of results obtained with the use of an impedance boundary condition in calculations of the scattering of surface plasmon polaritons by surface defects.

As a second example of the use of the approach developed in this paper, we consider the scattering of a surface plasmon polariton by a triangular groove or ridge. The surface profile function in this case is given by

$$\zeta(x_1) = -h + \frac{h}{a}|x_1| \quad 0 \leqslant |x_1| \leqslant a \tag{5.4a}$$

$$= 0 \quad |x_1| \geqslant a. \tag{5.4b}$$

When h is positive this function defines a groove; when h is negative it describes a ridge. The scattering of a surface plasmon polariton by a defect with this profile does not appear to have been studied by any approach until now. The function $J(\gamma|Q)$ obtained for this form for the surface profile function is

$$J(\gamma|Q) = -2\frac{a}{\gamma}\mathrm{sinc}(Qa) - \frac{2ah}{(\gamma h)^2 + (Qa)^2}e^{-\gamma h} + \frac{2a}{\gamma}\frac{1}{(\gamma h)^2 + (Qa)^2}(\gamma h \cos Qa + Qa \sin Qa), \tag{5.5}$$

where $\mathrm{sinc}x = \sin x/x$.

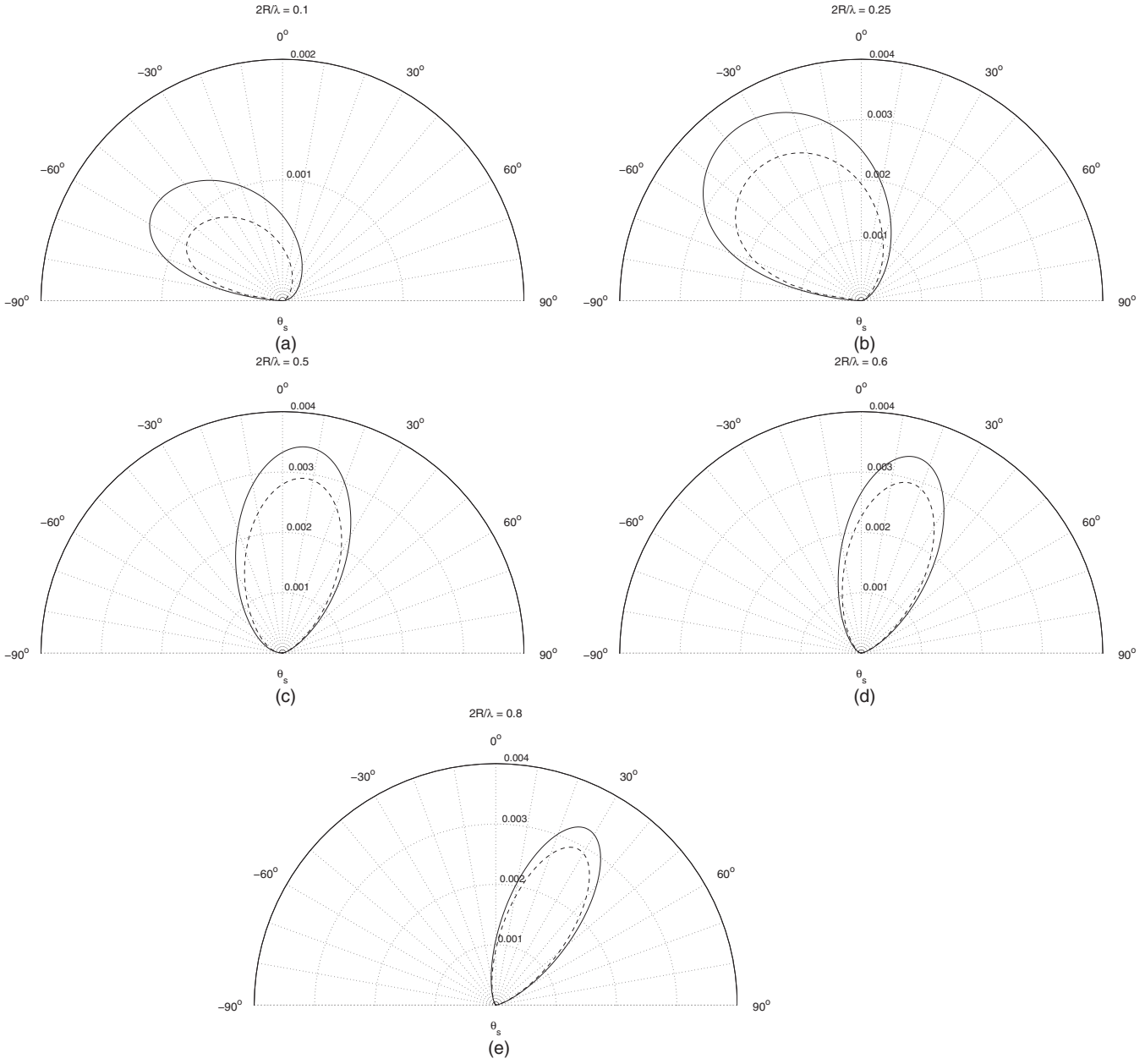

FIG. 6. The angular dependence of the emittance when a surface plasmon polariton whose wavelength is $\lambda = 600$ nm is incident normally on a Gaussian groove defined by Eq. (5.2) with $A = -12$ nm, on an otherwise planar silver surface. The values of $2R/\lambda$ assumed in obtaining these results are (a) 0.1, (b) 0.25, (c) 0.5, (d) 0.6, and (e) 0.8. In each case the solid curve (——) depicts the result obtained by the approach of this paper, while the dashed curve (- - - - -) depicts the result obtained in Ref. 17.

The functions $T(\omega), R(\omega), S(\omega)$, and their sum are plotted in Fig. 7 as functions of frequency for a triangular groove defined by $h = 40$ nm and $a = 250$ nm. If we compare these results with those presented in Fig. 1 for a Gaussian groove with the same depth and nearly the same width, we see that the ones in Fig. 7 display more structure, especially for ω just below $\omega_p/\sqrt{2}$. The transmittance has maxima and minima at the frequencies where the emittance has minima and maxima. The reflectance is again smaller than the transmittance and emittance by a factor of approximately one thousand. Unitarity is well satisfied by these results at frequencies up to $\omega/\omega_p \simeq 0.5$, and has an error no larger than about 2% at the highest frequencies.

The angular distribution of the emittance, $S(\theta_s)$, is presented in Fig. 8 for the case in which a surface plasmon polariton is incident normally on a triangular surface defect when the half width of the defect is fixed at the value $a = 250$ nm, while its amplitude $|h|$ assumes the values $|h| = 12$ nm, 40 nm, 60 nm, and 80 nm. The wavelength of the incident surface plasmon polariton is assumed to be $\lambda = 600$ nm. In contrast with the results presented in Fig. 4, it is seen in Fig. 8 that a triangular ridge converts more of the energy in the incident surface plasmon polariton into volume electromagnetic waves in the vacuum than does a groove, for each value of $|h|$. Moreover, for all the values of $|h|$ for which Fig. 8 was calculated, the radiation pattern has a maximum at a scattering angle $\theta_s = 10^\circ$.

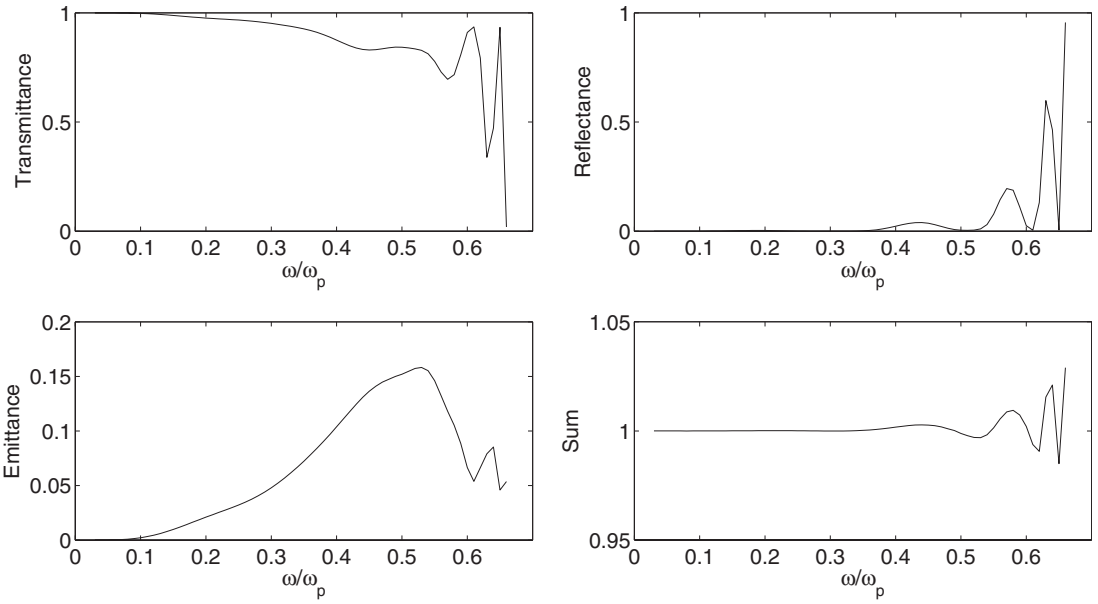

FIG. 7. The frequency dependence of the transmittance, reflectance, emittance, and their sum, when a surface plasmon polariton is incident normally on a triangular groove, defined by Eq. (5.4), on an otherwise planar silver surface. The values of the parameters assumed in obtaining these results are $\omega_p = 11.76 \times 10^{15}$ s^{-1}, $a = 250$ nm, and $h = 40$ nm.

The insensitivity of the scattering angle at which $S(\theta_s)$ has a maximum to the amplitude of the defect for a fixed value of its width seems to be a general property of one-dimensional topographical surface defects.

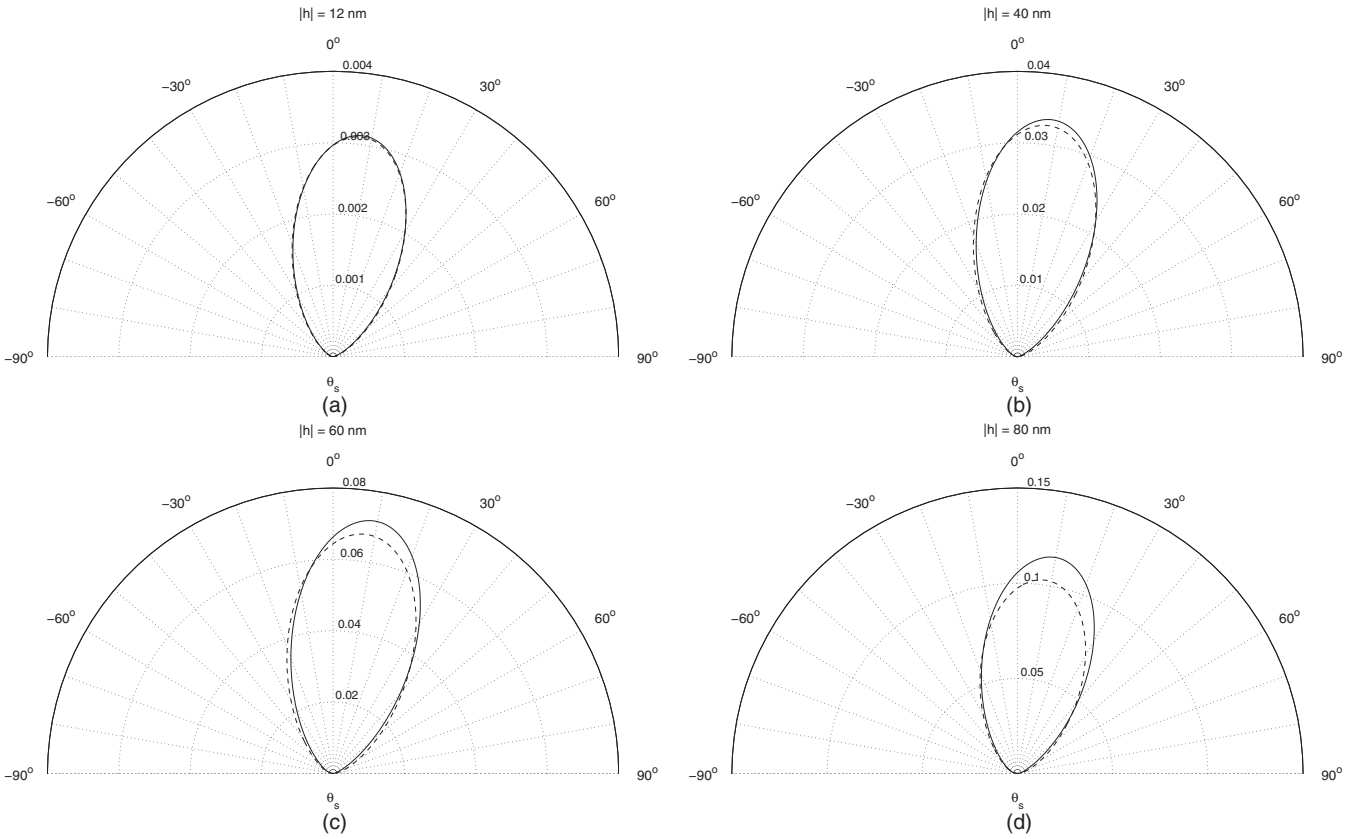

FIG. 8. The angular dependence of the emittance when a surface plasmon polariton whose wavelength is $\lambda = 600$ nm is incident normally on a triangular surface defect, defined by Eq. (5.4), on an otherwise planar silver surface. The values of the parameters used in obtaining these results are $\omega_p = 11.76 \times 10^{15}$ s^{-1}, $a = 250$ nm, and $|h| = 12$ nm (a), 40 nm (b), 60 nm (c), and 80 nm (d). In each case the solid curve depicts the result for a ridge, while the dashed curve depicts the result for a groove.

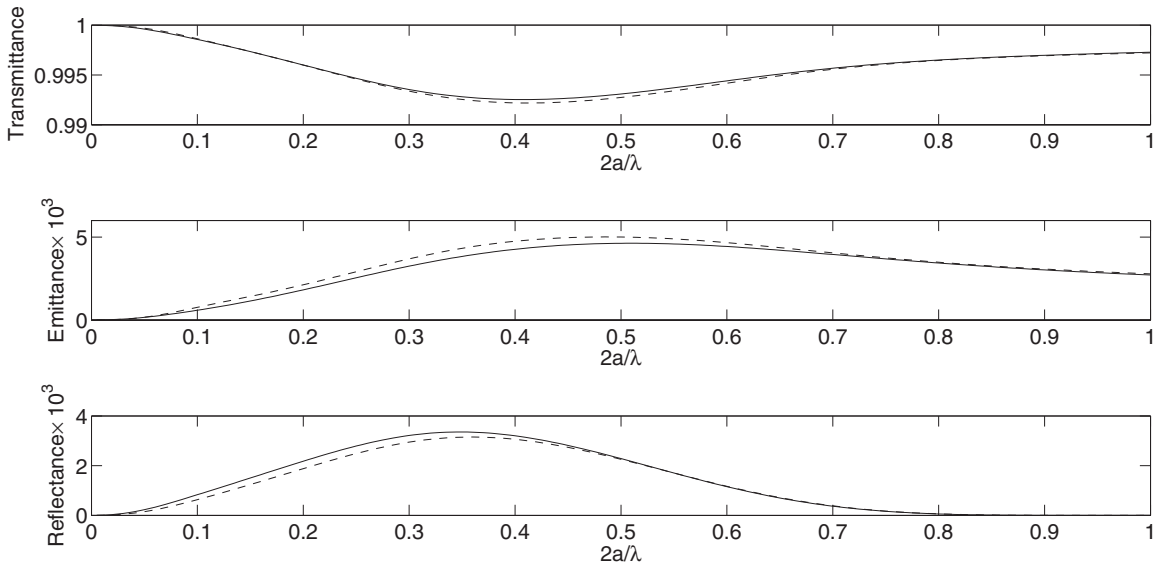

FIG. 9. The dependence of the transmittance, reflectance, and emittance of a triangular ridge or groove on an otherwise planar silver surface on $2a/\lambda$, when a surface plasmon polariton whose wavelength is $\lambda = 600$ nm is incident normally on it. The amplitude of the defect is $|h| = 12$ nm. The solid (——) and dashed (- - - -) curves in each case depict the results for a ridge and a groove, respectively.

In Fig. 9 we plot the dependence of the transmittance, reflectance, and emittance of the triangular defect as functions of its width when its amplitude is fixed, as is the wavelength of the incident surface plasmon polariton. The wavelength of the incident surface plasmon polariton is $\lambda = 600$ nm, and the amplitude of the defect is $|h| = 12$ nm. The transmittance is seen to be slightly larger for a ridge than for a groove, and to have a shallow minimum for $2a/\lambda \simeq 0.42$. The emittance and reflectance are both smaller than the transmittance by a factor of approximately one thousand for this shallow defect.

We conclude this section by presenting the angular dependence of the emittance, $S(\theta_s)$, when a surface plasmon polariton of wavelength $\lambda = 600$ nm is incident normally on a triangular surface defect, defined by Eq. (5.4) with $|h| = 12$ nm. The width of the defect $2a/\lambda$ takes the values 0.1, 0.25, 0.5, 0.6, and 0.8 in Figs. 10(a)–10(e), respectively. In each case the solid curve depicts the result for a ridge, while the dashed curve depicts the result for a groove. For values of $2a/\lambda$ up to about 0.7, the radiation is predominantly in the backward direction, while for values of $2a/\lambda$ larger than this value the radiation is predominantly in the forward direction. Scattering from a ridge yields a larger maximum value of $S(\theta_s)$ for small values of $2a/\lambda$, but for values of $2a/\lambda$ larger than 0.5 it is scattering from a groove that yields the larger maximum value of $S(\theta_s)$. Thus, for this surface profile as well altering the directionality of the emittance can be done by varying its width while keeping its amplitude fixed.

VI. DISCUSSION

In this paper we have first derived the reduced Rayleigh equation for the scattering of a surface plasmon polariton incident normally on a one-dimensional topographical defect on an otherwise planar metal surface in contact with vacuum. We have then applied this equation to the determination of the scattering coefficients for defects defined by a Gaussian profile function and by a symmetric triangular profile function. Two assumptions underlie the present work, namely that the use of the Rayleigh hypothesis is valid, and that the dielectric function can be assumed to be real. We consider these two assumptions in turn.

The conditions for the validity of the Rayleigh hypothesis have been studied by many authors.[26–33] Hill and Celli[28] have presented a simple method for determining the limits of validity of Rayleigh's method, while van den Berg and Fokkema[30] have used a somewhat different approach to determine these limits for a one-dimensional perturbation of a planar surface. The latter authors have determined these limits for a surface defect defined by the profile function given by Eq. (5.2). They find that for $A > 0$ the Rayleigh hypothesis is valid for $0 < A/R < 0.429$, while for $A < 0$ it is valid for $-0.694 < A/R < 0$. Thus the Gaussian profiles we have studied are defined by values of A/R for which the Rayleigh hypothesis is valid. The results presented here can therefore be regarded as having been obtained by means of rigorous calculations.

The situation with respect to the triangular surface defect defined by the profile function (5.4) is subtler. If a surface profile function is not an analytic function of x_1, for example if it has corners, then according to a theorem of Millar[27] in general the Rayleigh hypothesis is not valid.[28,34] However, it has been found by several authors that the Rayleigh method yields accurate results even when it is used outside its domain of analytical validity, and when it is applied to nonanalytic surface profile functions in calculations of the dispersion curves for surface waves propagating across periodically corrugated surfaces.[35–37] It has been suggested that the accuracy of the method outside its domain of validity is asymptotic in nature.[28,38] By this is meant that the accuracy of

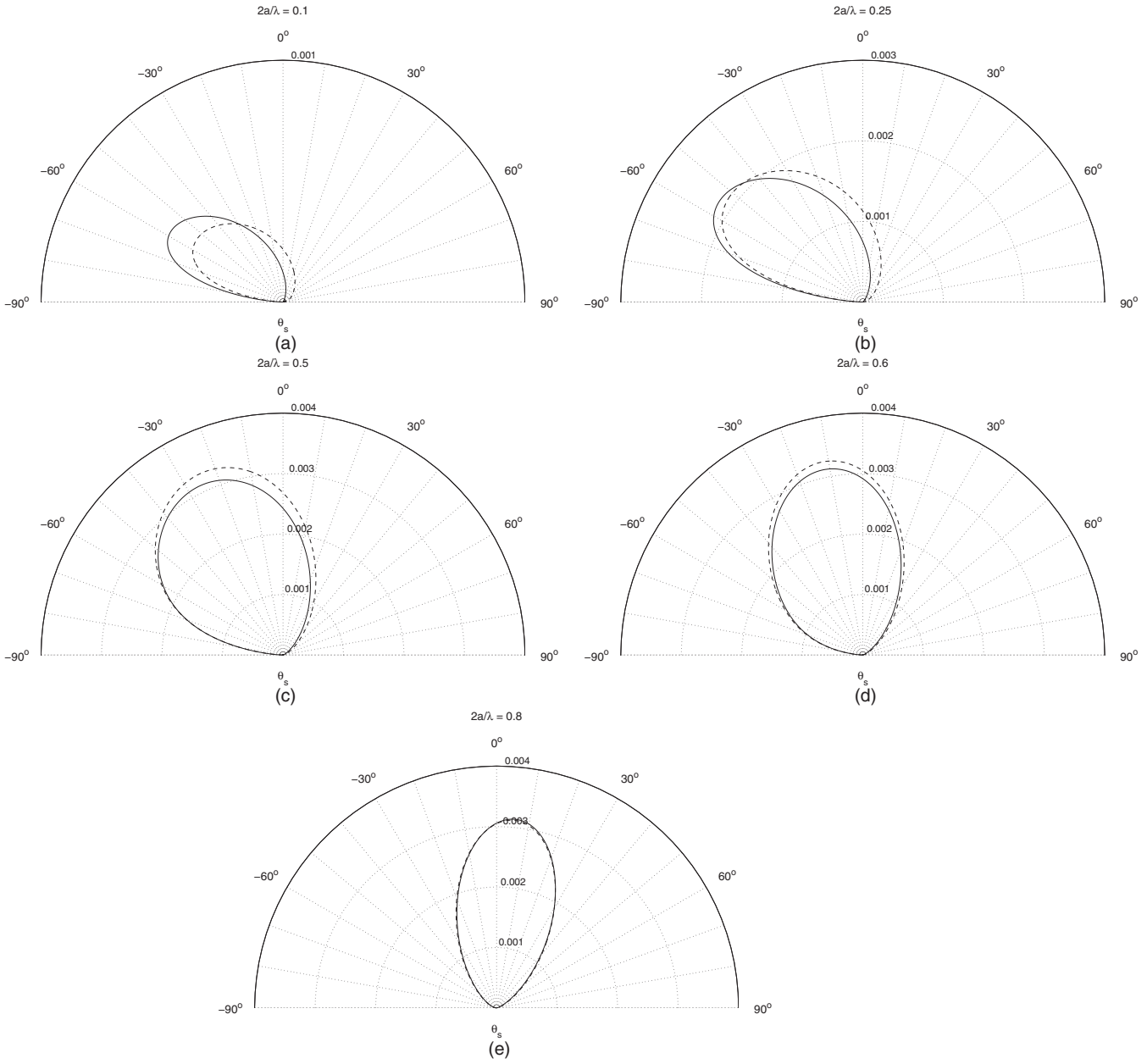

FIG. 10. The angular dependence of the emittance when a surface plasmon polariton whose wavelength is $\lambda = 600$ nm is incident normally on a triangular surface defect, defined by Eq. (5.4) with $|h| = 12$ nm, on an otherwise planar silver surface. The values of $2a/\lambda$ assumed in obtaining these results are (a) 0.1, (b) 0.25, (c) 0.5, (d) 0.6, and (e) 0.8. In each case the solid curve (——) depicts the result for a ridge, while the dashed curve (- - - - -) depicts the result for a groove.

the result calculated (surface wave dispersion curve, scattering efficiency) improves as the number of terms in the expansion of the scattered wave in terms of outgoing wave functions is increased up to some critical value, and then worsens as additional terms are included. In the present case of an isolated surface defect summation over outgoing wave functions is replaced by integration. It was found that as the interval of integration $(-Q, Q)$ in the numerical solution of Eq. (2.16) is expanded by increasing Q, the result for the scattering amplitude improves until a critical value of Q is reached, and then worsens as Q is increased beyond this value. We have always used results obtained with this critical value of Q.

We now turn to a discussion of the assumption the the dielectric function $\epsilon(\omega)$ of the metal can be taken to be real. This assumption is justified when the energy mean free path of a surface plasmon polariton on a lossy metal surface is so long that the component of the Poynting vector of the surface wave in the direction of its propagation decreases so little in its transit of the defect that results for a lossless metal can be used instead.

To make this argument quantitative, we write $\epsilon(\omega)$ in the form $\epsilon(\omega) = \epsilon_1(\omega) + i\epsilon_2(\omega)$, where $\epsilon_1(\omega)$ is negative while $\epsilon_2(\omega)$ is positive in the frequency range of interest. The energy mean free path of a surface plasmon polariton of frequency ω

at a planar vacuum-metal interface is then given by

$$\ell_{\rm spp}(\omega) = \frac{c}{\omega}\frac{|\epsilon_1(\omega)|^{\frac{1}{2}}(|\epsilon_1(\omega)|-1)^{3/2}}{\epsilon_2(\omega)}. \tag{6.1}$$

The dielectric function of silver at a wavelength $\lambda = 2\pi c/\omega = 600$ nm, obtained by a linear interpolation of data in the paper of Johnson and Christy[39] is $\epsilon(\omega) = -15.91 + i0.435$. This result for the real part of $\epsilon(\omega)$ differs from the value of -19.41 used in Ref. 17, but this difference is not significant for our argument. The value of $\ell_{\rm app}(\omega)$ obtained from this value of $\epsilon(\omega)$ and Eq. (6.1) is $\ell_{\rm spp}(\omega) = 51.63\,\mu$m. This is more than 100 times larger than the widths of our defects, which in most of our examples are 500 nm. This result means that the surface plasmon polariton loses less than one percent of the energy with which it enters the defect as it transits the defect. If the reflectance and transmittance of the surface plasmon polariton are calculated in terms of the values of the 1-component of the Poynting vector of the reflected and transmitted fields evaluated at the entrance and exit points of the defect, respectively,[19] the errors in the calculations of these functions with a real dielectric function instead of a complex one should be smaller than one percent.

We have studied quantitatively how the frequency dependence of the transmittance, emittance, and reflectance of a ridge differ from those of a groove for a Gaussian surface defect, and have found that these differences are in fact very small. The frequencies at which the spectral dependencies of the transmittance, emittance, and reflectance have their minima or maxima are only very weakly dependent on the values of the parameters A and R that define this surface defect. The spectral dependencies of these functions for a triangular groove have more structure than those for the Gaussian defect, especially in the high frequency limit. The accuracy of these calculations decreases as ω/ω_p increases past $\omega/\omega_p = 0.66$.

The angular dependencies of the emittance for a ridge and a groove are quite close to each other for a Gaussian defect, and a little less so for the triangular defect. The emittance is in the forward direction for each value of $|A|$ and $|h|$ for the Gaussian and triangular defects, respectively, and although its strength increases as the amplitude of the defect increases with its width held constant, the scattering angle at which the emittance is a maximum is independent of the magnitude of the amplitude. This result suggests that the excitation of a surface plasmon polariton by illuminating a Gaussian or triangular ridge or groove by a p-polarized volume electromagnetic wave incident from the vacuum will be most efficient when the polar angle of incidence equals the angle at which the emittance is a maximum.[40]

When we fix the frequency (wavelength) and the magnitude of the amplitude of the Gaussian or triangular defect while we increase the width of the defect, we find that the transmittance has a single broad minimum while the emittance and the reflectance each have a single broad maximum. In the case of the Gaussian defect, with the choices $\lambda = 600$ nm and $|A| = 12$ nm, we can compare our results with those of Ref. 17, which were obtained by the use of an impedance boundary condition. There is a qualitative agreement between the two sets of results for the ridge and the groove, and semiquantitative agreement. The quantitative agreement is best for the results for a ridge, but less good for a groove.

Similar results are obtained for the angular dependence of the emittance when a surface plasmon polariton of a fixed frequency is incident on a Gaussian groove of fixed depth and variable width. The results obtained by the present approach are in qualitative agreement with those obtained in Ref. 17, but the latter results are systematically smaller than the former. The width of the groove at which the emittance changes from being primarily in the backward direction to being primarily in the forward direction is the same in the results obtained by our approach and by the one of Ref. 17.

When we fix the wavelength of the incident surface plasmon polariton and the magnitude of the amplitude of the triangular surface defect while its width is increased, the angular dependence of the emittance is qualitatively similar to that for a Gaussian defect. For small values of the width the emittance is primarily in the backward direction, with the ridge producing the greater maximum intensity. As the width of the defect is increased the emittance becomes primarily in the forward direction, with the greater maximum intensity now being produced by the groove. Thus, again the radiation pattern can be controlled by varying the width of the defect.

Although the approach developed here can be applied to studies of the scattering of a surface plasmon polariton by multiple, parallel, one-dimensional surface defects, or to the scattering of a surface plasmon polariton pulse from one or more surface defects, we have applied it here to the case of a single surface defect. We plan to study extensions of the present study to multiple defects and pulses in subsequent work.

In conclusion, we have developed an approach to the study of the scattering of surface plasmon polaritons by one-dimensional topographic surface defects on a planar surface that is correct, accurate, and computationally simple to implement, even if it has some limits on its applicability, as long as it is used within these limitations, and in some cases even outside these limitations. It is based on the method of reduced Rayleigh equations, a method that has been used successfully in many studies of various properties of structured metallic, dielectric, elastic, and magnetic surfaces. We have compared some of the results obtained by this approach with those obtained by a different earlier approximate approach and have obtained good agreement with them, which provides a kind of independent confirmation of those earlier results. Among our new results the most striking is the insensitivity of the directionality of the emittance to variations of the amplitude of the defect for a fixed value of its width. This result has a useful consequence for the excitation of a surface plasmon polariton by illuminating such a defect by a volume electromagnetic wave.

ACKNOWLEDGMENTS

We are very grateful to A. Yu. Nikitin for sending us the results plotted in Figs. 2 and 3 of Ref. 17 which made possible comparisons of our results with those of that reference. The research of J.P. and R.M.F. was supported in part by NOAA Educational Partnership Program for Minority Serving Institutions (EPP/MSI) Cooperative Agreement NAITAE1523. The research of A.A.M. was supported in part by AFRL Contract No. FA9453-08-C-0230.

[1]A. V. Zayats, I. I. Smolyaninov, and A. A. Maradudin, Phys. Rep. **408**, 131 (2005).
[2]I. I. Smolyaninov, C. C. Davis, and A. V. Zayats, New J. Phys. **7**, 175 (2005).
[3]I. I. Smolyaninov, D. L. Mazzoni, and C. C. Davis, Phys. Rev. Lett. **77**, 3877 (1996).
[4]V. Bohnsen and S. I. Bozhevolnyi, Appl. Opt. **40**, 6081 (2001).
[5]Z. Liu, J. M. Steele, W. Srituravanich, Y. Pikus, C. Sun, and X. Zhang, Nano Lett. **5**, 1726 (2005).
[6]J. Y. Lee, B. H. Hong, W. Y. Kim, S. K. Min, Y. Kim, M. V. Jouravlev, R. Bose, K. S. Kim, I.-C. Hwang, L. J. Kaufman, C. W. Wong, P. Kim, and K. S. Kim, Nature (London) **460**, 498 (2009).
[7]A. V. Shchegrov, I. V. Novikov, and A. A. Maradudin, Phys. Rev. Lett. **78**, 4269 (1997).
[8]E. Kretschmann, Z. Phys. **241**, 313 (1971).
[9]M. Paulus and O. J. F. Martin, J. Opt. Soc. Am. A **18**, 854 (2001).
[10]B. Baumeier, F. Huerkamp, T. A. Leskova, and A. A. Maradudin, Phys. Rev. A **84**, 013810 (2011).
[11]J. A. Sánchez-Gil, Appl. Phys. Lett. **73**, 3509 (1998).
[12]J. A. Sánchez-Gil and A. A. Maradudin, Phys. Rev. B **60**, 8359 (1999).
[13]J. A. Sánchez-Gil and A. A. Maradudin, Opt. Lett. **28**, 2255 (2003).
[14]J. A. Sánchez-Gil and A. A. Maradudin, Opt. Express **12**, 883 (2004).
[15]J. A. Sánchez-Gil and A. A. Maradudin, Appl. Phys. Lett. **86**, 251106 (2005).
[16]A. A. Maradudin, in *Topics in Condensed Matter Physics*, edited by M. P. Das (Nova Science Publishers, New York, 1994), pp. 33–45.
[17]A. Y. Nikitin, F. López-Tejeira, and L. Martín-Moreno, Phys. Rev. B **75**, 035129 (2007).
[18]A. Yu. Nikitin and L. Martín-Moreno, Phys. Rev. B **75**, 081405(R) (2007).
[19]T. A. Leskova, A. A. Maradudin, E. E. García-Guerrero, and E. R. Méndez, Fiz. Nizk. Temp. **36**, 1022 (2010).
[20]I. Chremmos, J. Opt. Soc. Am. A **27**, 85 (2010).
[21]G. Brucoli and L. Martín-Moreno, Phys. Rev. B **83**, 045422 (2011).
[22]G. Brucoli and L. Martín-Moreno, Phys. Rev. B **83**, 075433 (2011).
[23]M. Kuttge, F. J. García de Abajo, and A. Polman, Opt. Express **17**, 10385 (2009).
[24]F. Toigo, A. Marvin, V. Celli, and N. R. Hill, Phys. Rev. B **14**, 5618 (1977).
[25]Lord Rayleigh, *The Theory of Sound*, 2nd ed., Vol. II (MacMillan, London, 1896), pp. 89, 297–311.
[26]R. Petit and M. Cadilhac, C. R. Acad. Sci. B **262**, 468 (1966).
[27]R. F. Millar, Proc. Cambridge Philos. Soc. **65**, 773 (1969).
[28]N. R. Hill and V. Celli, Phys. Rev. B **17**, 2478 (1978).
[29]P. M. van den Berg and J. T. Fokkema, J. Opt. Soc. Am. **69**, 27 (1979).
[30]P. M. van den Berg and J. T. Fokkema, Radio Sci. **15**, 723 (1980).
[31]W. A. Schlup, J. Phys. A: Mathematical and General **17**, 2607 (1984).
[32]J. A. De Santo, Radio Sci. **16**, 1315 (1981).
[33]T. C. Paulick, Phys. Rev. B **42**, 2801 (1990).
[34]R. F. Millar, Radio Sci. **8**, 785 (1973).
[35]B. Laks, D. L. Mills, and A. A. Maradudin, Phys. Rev. B **23**, 4965 (1981).
[36]A. A. Maradudin and N. E. Glass, Electron. Lett. **17**, 773 (1981).
[37]N. E. Glass, R. Loudon, and A. A. Maradudin, Phys. Rev. B **24**, 6843 (1981).
[38]F. O. Goodman, J. Chem. Phys. **66**, 976 (1977).
[39]P. B. Johnson and R. W. Christy, Phys. Rev. B **6**, 4370 (1972).
[40]M. Kretschmann, T. A. Leskova, and A. A. Maradudin, Proc. SPIE **4447**, 24 (2001).